Springer

KSME

Journal of Mechanical Science and Technology 32 (6) (2018) 2735~2746
www.springerlink.com/content/1738-494x(Print)/1976-3824(Online)
DOI 10.1007/s12206-018-0530-0

Flexible CNC polishing process and surface integrity of blades †

Xiaojun Lin[1,*], Dongbo Wu[1], Xiufeng Shan[1], Gang Wu[1], Tong Cui[1], Yun Zhang[1], Liangyi Hu[2] and Jie Yu[2]

[1]*The Key Laboratory of Contemporary Design and Integrated Manufacturing Technology, Ministry of Education, Northwestern Polytechnical University, Xi'an 710072, China*
[2]*AECC Xi'an Aero-engine Ltd., Xi'an, Shaanxi 710021, China*

(Manuscript Received June 26, 2017; Revised February 7, 2018; Accepted March 14, 2018)

Abstract

The surface integrity of aero-engine blades directly affects its mechanical behavior. To improve the surface integrity and address the problem, that is, the blade is mainly polished manually, a flexible polishing process was proposed and surface integrity was investigated. First, flexible polishing technology and the machine tool that the authors researched and developed were introduced. Second, a polishing experiment was conducted on a TC4 titanium alloy blade. Finally, the surface integrity before and after polishing was measured and the results were compared and analyzed. Results showed that the knife marks, pits, unevenness, and other defects of the blade surface were effectively removed through flexible polishing; the surface residual compressive stress was reduced from 483 MPa to 397 MPa; the surface roughness was reduced to Ra 0.4 μm; the surface micro-hardness increased by 18 HV; and the surface metamorphic layer caused by milling was removed. Flexible polishing effectively improved the surface quality without affecting the depth layer quality of the workpiece.

Keywords: TC4 titanium alloy; Blade; Flexible polishing; Surface integrity

1. Introduction

Aircraft engines utilize blades to complete gas compression and expansion and generate sufficient power to propel the aircraft. Such blades are special mechanical parts of aircraft engines due to their large number, complex shapes, high performance, difficulty in mechanical processing, and failure propensity. Thus, blade production is crucial in engine plants.

Titanium is widely used in manufacturing aero-engine blades due to its high specific strength, high temperature resistance, and corrosion resistance. TC4 titanium alloy is a common material. Fatigue failure begins with surface defects, such as cutting tool mark, uneven residual stress distribution, and surface tissue damage. These defects are caused by local tensile stress superposition on the fatigue load, which considerably promote fatigue crack initiation that results in the drastic reduction of the fatigue strength of blades and loss of fatigue life. The fatigue performance of blades highly depends on surface integrity, whose main characterization parameters are surface roughness, surface topography, residual stress, microhardness, and microstructure. Therefore, controlling surface integrity is critical in improving fatigue resistance, and surface polishing technology is the most effective and widely used surface processing technology.

At present, considerable works on polishing methods and polishing surface integrity have been conducted with corresponding results. Axinte et al. [1, 2] studied the effects of different polishing parameters on the surface integrity of titanium alloy using the abrasive belt polishing process. Rech et al. [3] established a belt grinding model and analyzed the influence of belt polishing on residual stress. Tam et al. [4] studied the effect of polishing path on material removal rate in silicon wafer polishing through simulation and experiment, and the results showed that tool path and path line change directions had a significant effect on surface roughness. Hung et al. [5] investigated the effect of particle size and tool type on grinding tool wear rate during grinding. Lee et al. [6] experimentally investigated the influence of tray and chuck speed on the surface roughness of silicon wafer during water jet polishing. The experimental results showed that the processing speed affected the processing temperature. Jourani et al. [7] studied the relationship between the structure of abrasive belt and surface quality, analyzed the physical mechanism of abrasive belt grinding, established a mathematical model of surface material removal, and improved the workpiece surface integrity by controlling the grinding process of abrasive belt. Ek-

*Corresponding author. Tel.: +29 88460426, Fax.: +29 88460426
E-mail address: linxj@nwpu.edu.cn
† Recommended by Associate Editor In-Ha Sung

kard et al. [8] proposed a new method of polishing technology using nylon needle or wheel polishing tool. They analyzed the influence factors of surface roughness and material removal and indicated that the polishing tool, workpiece relative speed, and polishing pressure were the main factors that affect surface quality. Bigerelle et al. [9-12] proposed a characterization method of surface roughness in the wear and tear of tools and characterized the surface integrity, machining dynamics, and mechanical properties using a series of roughness parameters. They also established a fractal model of the wear rate in the polishing process and a polishing process model. Hamdi et al. [13] studied residual stress calculation in polishing process and analyzed the effect of thermal–mechanical coupling on the residual stress of the surface of a workpiece. Odén et al. [14] studied the relationship among surface integrity, bending strength, and grinding on WC–Co cemented carbide, which is a tungsten carbide material. The study showed that grinding could significantly affect the surface integrity and bending strength of workpieces. Tsai et al. [15] established a prediction model of grinding surface roughness on the basis of an adaptive genetic algorithm, which effectively improved the surface roughness of grinding. Han et al. [16] constructed a research model for multiple discrete silicon nitride polishing process of polysilicon by using discrete element method and determined the relationship between ceramic mechanical polishing and surface integrity model. Klocke et al. [17] proposed a modeling method on the basis of the broaching method for the temperature stress of nickel-based alloys to predict surface integrity and control the surface quality of workpieces during machining.

Huang et al. [18] conducted considerable research on abrasive belt polishing technology and tested the polishing process of stainless steel and titanium alloy workpiece on the developed belt grinding machine. On this basis, they analyzed the influence of the belt speed, grinding pressure, contact wheel hardness, types of abrasive belt, material characteristics of workpieces and polishing dosage, and other parameters on belt life, belt wear, material removal rate, and surface roughness. Ji et al. [19] proposed a new type of gasbag polishing technique based on the concept of flexible polishing; they built a corresponding robot polishing system and studied the rotary expansion gasbag polishing tool and the influence of various factors on polishing surface roughness in the polishing process. Guo et al. [20] developed a free surface magnetic grinding device based on a robot, performed machining test on integral bladed disk, and examined the polished surface quality from surface roughness, microstructure, micro crack, microstructure, and residual stress. Zhang et al. [21] studied the effects of grinding parameters on surface integrity, established an empirical formula for surface roughness, analyzed the sensitivity of surface roughness to grinding parameters, and obtained the stable and unstable domains of grinding parameters. Yao et al. [22] conducted the cutting experiments on TB6 titanium alloy and investigated the effects of high-speed cutting parameters on surface characteristics in terms of surface integrity.

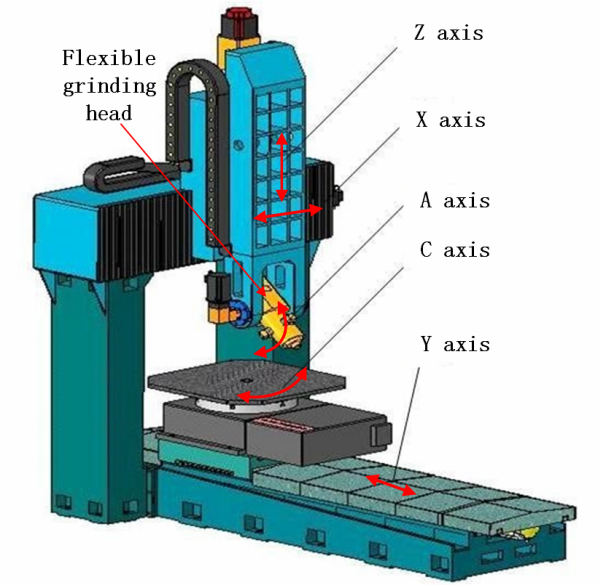

Fig. 1. Structure of polishing machine tool.

The authors found that 5-axis 5-linkage CNC abrasive cloth wheel polishing was feasible; they designed and developed a 5-axis 5-linkage CNC flexible abrasive cloth wheel polishing machine tool [23] and studied its polishing process [24]. The concept of effective contact between the polishing wheel and complex workpiece surface was proposed; the effective contact was successfully achieved by improving the polishing tool and controlling the polishing shaft vector and optimizing flexible polishing; and polishing process parameters were selected using parameter optimization experiment with the surface roughness as the optimization target. The polishing method is currently in the exemplary application stage.

On this basis, the present study uses the typical complex free surface parts—aero-engine TC4 titanium alloy blade as the research object—in performing polishing experiments on the machine tool that the authors researched and developed. The flexible polishing CNC process and surface integrity are studied, and the influence of flexible polishing process on surface roughness, microstructure, residual stress, microhardness, and microstructure is explored.

2. Flexible polishing principle and machine

Polishing experiments were conducted on the YPGZ-1000 5-axis 5-linkage CNC abrasive cloth wheel polishing machine tool, which was researched and developed by the authors, as shown in Fig. 1.

The equipment is composed of three linear axes X, Y and Z and two rotary axes C and A. Axes X, Z and A complete the straight and rotation trajectory control of the abrasive cloth wheel mechanism, respectively, whereas axes Y and C complete the straight and rotation trajectory control of the workpiece, respectively. The collaboration of the five axes, called

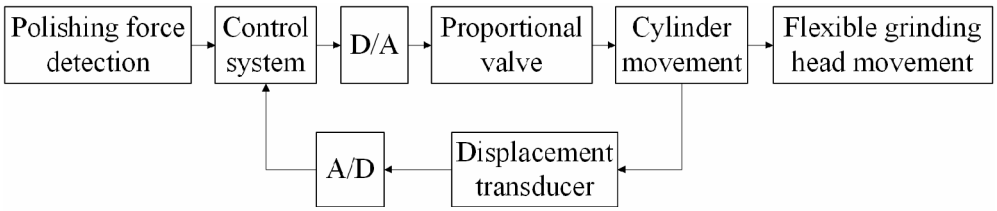

Fig. 2. Adaptive control flow chart of polishing equipment.

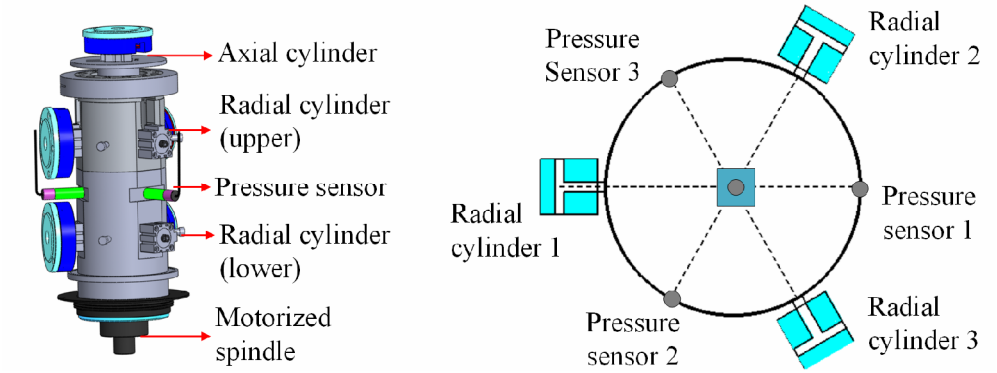

(a) Internal structure (b) Schematic diagram

Fig. 3. Structure of flexible head.

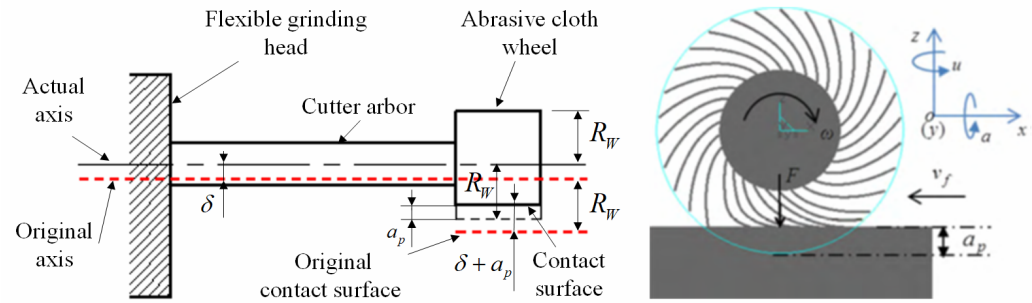

Fig. 4. Flexible principle.

5-axis 5-linkage, completes the polishing of the complex surface blade.

Polishing principle is self-adaptive and flexible. Self-adaptive flexible polishing is an engineering technique wherein the flexible polishing tool can make flexible actions based on the shape change of the workpiece. The flexible action is either from the elastic deformation of the polishing tool or the control of the flexible polishing mechanism. Its flexible feature emphasizes on the adaptability of the polishing tool and polishing mechanism to the geometrical shape of free surface.

The self-adaptive control flowchart of the polishing equipment is shown in Fig. 2. The industrial control system initially determines the required amount of the minor adjustments of the grinding head by polishing force detection and force data collection. Finally, the industrial control system manages the protrusion and retraction of the air cylinders by changing the pressure output of the proportional valve to finish the micro-movement of the grinding head. The position of the grinding head is determined by the value of the protrusion and retraction volume of the air cylinders collected by the industrial control system via displacement sensors. Hence, the industrial control system can accomplish the online measurement and error feedback compensation of the grinding head position and the polishing force to achieve blade self-adaptive polishing.

Fig. 3 shows the internal structure and schematic of the flexible head. Three sets of cylinders are uniformly distributed along the radial direction of the flexible head. In addition, each set consists of upper and lower cylinders. The cylinders are used to complete the motion of the motorized spindle. Moreover, a pressure sensor is installed on the opposite direction of each cylinder set, which is used to test the pressure data of the motorized spindle. The contact force can be adjusted using the coordinated motion of the three cylinders sets.

Flexibility is mainly classified into two aspects. First, the flexible grinding head allows the spindle to shift slightly in a cycle with a radius of R via the radially distributed three air cylinders. Second, radial deformation occurs in the abrasive

cloth wheel under the influence of contact force. The polishing state diagram is shown in Fig. 4. In the figure, δ represents the deviation between the actual working axis of the spindle and the original axis, and a_p represents the deformation of abrasive cloth wheel. Therefore, the total radial deviation between the working plane and the plane where the abrasive cloth wheel only contacts the workpiece is the sum of two parameters, δ and a_p, which is expressed in Eq. (1).

$$L = \delta + a_p . \tag{1}$$

In actual polishing, L can be adjusted flexibly based on the polishing process to achieve flexible contact between the abrasive cloth wheel and the workpiece. The total deviation L can be understood as the displacement of the tool, which not only reduces the machining deformation of the workpiece and the stress concentration in the machining zone but also avoids the machining impact phenomenon in rigid contact. Flexible polishing requires minor adjustments of the polishing force and increases the contact area between the workpiece and the abrasive cloth wheel.

3. Experiment schemes

The material used in the experiment was TC4 titanium alloy. This alloy has excellent corrosion resistance, small density, high specific strength, superior toughness, and advanced weldability and has been successfully used in aerospace, petrochemical, shipbuilding, automotive, and pharmaceutics. Specifically, this alloy has been extensively used in aero-engine blades. Table 1 shows the chemical compositions of TC4 titanium alloy, and Table 2 shows its main mechanical properties.

The blade profile is a complex free-form surface part (Fig. 5). The size of this blade surface is approximately 60 mm × 60 mm, and the maximum thickness is 2 mm. This blade is a small one compared with the larger aero-engine fan blade. The blade consists of rabbet, blade root, and blade body and is classified into concave and convex. The concave and convex blades are the main polished parts. In this work, the polishing experimental surface used is the concave surface.

Aero-engine blade processing technology consists of the following steps: rough, semi-finished, and finished millings and polishing. The precision milling is accomplished using the VMC 850 CNC machine tool. Polishing is the last step, which requires the surface roughness of the milled specimen. Generally, the surface roughness of precision milled specimen should achieve the range of Ra 1.0–1.4 μm. Wheel grinding is a commonly used method; however, the surface integrity after wheel grinding undergoes tremendous changes, because the large grinding force and grinding heat result in large heat–force coupling, which induces complex heat transfer and mass transfer phenomenon. Hence, these phenomena will be reflected in the surface integrity of the workpiece. The characterization parameters of surface integrity, such as surface roughness, surface topography, residual stress, micro-hardness, and microstructure, will change.

Table 1. Chemical composition of TC4 titanium alloy.

Al	V	Fe	Si	C	N	H	O
5.5–6.8	3.5–4.5	0.30	≤ 0.15	≤ 0.10	≤ 0.05	≤ 0.01	≤ 0.20

Table 2. Mechanical properties of TC4.

Yield stress σb (MPa)	Elongation δ (%)	Impact value a_k (J/cm^2)	Thermal conductivity λ (J/cm·s·°C)
932	10	39.24	0.068

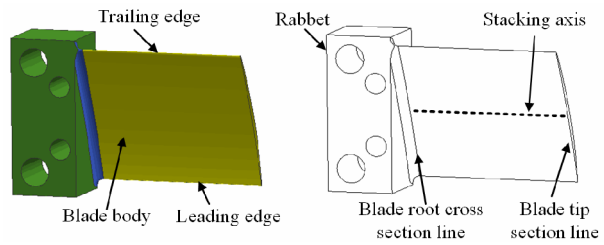

Fig. 5. Titanium alloy blade structure.

Flexible polishing, compared with grinding wheel grinding, has a clear feature, that is, the flexible polishing heat and force are relatively small and the polishing force is self-adaptable and controllable. Flexible polishing is a process of repeated polishing that results in the accumulation of polishing force and temperature and affects surface integrity. Repeated polishing increases the polishing times, which reduces polishing efficiency. The results of the experiments show that the number of polishing times does not affect the shape accuracy of the workpiece and that the shape accuracy of the workpiece polished 4, 8 and 12 times meets the requirements. These results are caused by the main purpose of flexible polishing compared with milling, which is to improve the surface quality of the workpiece rather than removing the material margin; moreover, the change of the shape accuracy and material removal is minimal. Therefore, studying the change of surface integrity under different polishing times is necessary. The research steps are shown as follows.

Step 1: Complete the milling experiment and obtain the three specimens by using the same milling parameters 1#, 2# and 3#.

Step 2: The surface roughness, surface topography, residual stress, micro-hardness, and microstructure of the milled workpiece are measured.

Step 3: The 1#, 2# and 3# specimens are polished 4, 8 and 12 times, respectively, on the basis of the optimization polishing process parameters.

Step 4: The surface roughness, surface topography, residual stress, micro-hardness, and microstructure of the polished workpiece are measured, and the results are compared with the result of milled workpiece.

4. Experimental conditions and procedure

A sample of 10 mm × 10 mm × 2 mm on the blade processing area is cut to analyze the effect of flexible polishing on surface integrity. The contrast experiments are conducted between the milled and polished blade surfaces in terms of surface roughness, surface topography, residual stress, microhardness, and microstructure.

Blade polishing. The blade is polished on the 5-axis 5-linkage CNC abrasive cloth wheel polishing machine tool (Fig. 6). The convex and concave surfaces are polished separately. The polishing method is divided into longitudinal and horizontal polishing. The path of the longitudinal polishing is perpendicular to the direction of the stacking axis, whereas the path of the horizontal polishing is along the direction of the stacking axis. The method used in this study is longitudinal polishing, whose path is shown in Fig. 7(b).

The reason is that longitudinal polishing cannot cause polishing lines along the stacking axis on the blade, which negatively affect the anti-fatigue properties of the blade. Table 3 shows the polishing process parameters used in this study. The polishing tool used is an abrasive cloth wheel, which mainly comprises a mandrel, pieces of the abrasive belt, and blinder (Fig. 7(b)). The mandrel, which is made of polypropylene, is a drilled thread hole used to fix the abrasive cloth wheel on the flexible grinding head with the steel handle (Fig. 7(b)). Its processing condition is dry polishing. The workpiece is fixed to the rotary table by using clamps (Fig. 6).

Surface roughness and topography. MarSurf M300C is used to measure the surface roughness. First, three points along the stacking axis direction in region A on the milled surface are selected. Second, each selected point is tested three times. Finally, the average of the three values is calculated as the surface roughness value of this point to meet the statistical significance of the measurement. The measuring length is 0.8 mm, and the assessment length is 5.6 mm.

Surface topography is measured using Alicona-Automatic optical test instrument on the milled surface. The magnification is 5×, and the measuring range is 0.4 mm × 0.4 mm.

The surface roughness and topography measurement method of the polished surface is the same. Fig. 8 shows the test site.

Residual stress. The residual stress is measured using PROTO LXRD MG2000 residual stress test analysis system. First, the instrument is calibrated using a titanium alloy block before performing the measurement. Second, three equidistant points along the stacking axis direction in region B on the milled surface are selected (Fig. 8). Third, the surface residual stress in the x- and y-directions of each selected point is tested three times. Fig. 9 shows the test site. Finally, the average of the three values is calculated as the surface residual stress value of this point to meet the statistical significance of the measurement.

To obtain the residual stress distribution along the depth direction, the specimens are stripped using electrochemical method, and the stripping depth is 10 μm. The residual stress is alternately tested until the result is close to the body material's residual stress by repeated stripping. PROTO LXRD MG2000 is also used as the residual stress measurement tool of the polished surface.

Micro-hardness. Micro-hardness is measured using FEM-8000 semi-automatic digital micro-hardness testing system. First, a sample of 10 mm × 10 mm × 2 mm on the blade processing area is cut and mounted on the embedded machine. The

Table 3. Polishing process parameters.

Granularity of abrasive cloth wheel	Speed n (rpm)	Feed rate v (mmpm)	Compression amount a_p (mm)
1000	6000	250	0.3

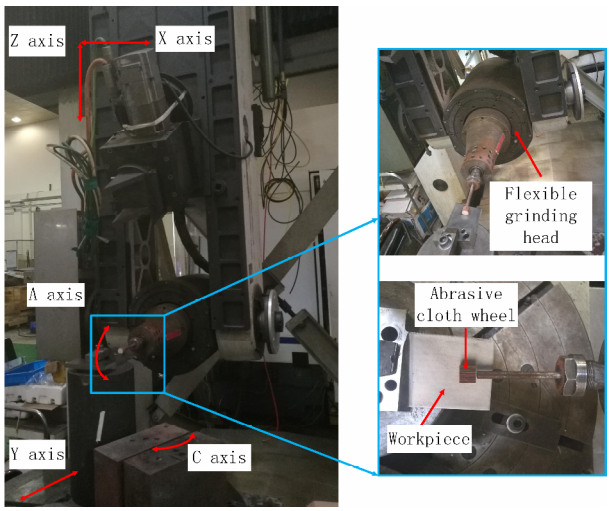

Fig. 6. Experimental setup for blade polishing.

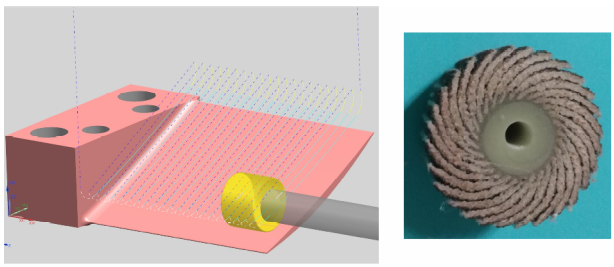

(a) Polishing path (b) Abrasive cloth wheel

Fig. 7. Abrasive cloth wheel and polishing path.

(a) Test area (b) Measuring instrument

Fig. 8. Surface roughness measuring instrument and test area.

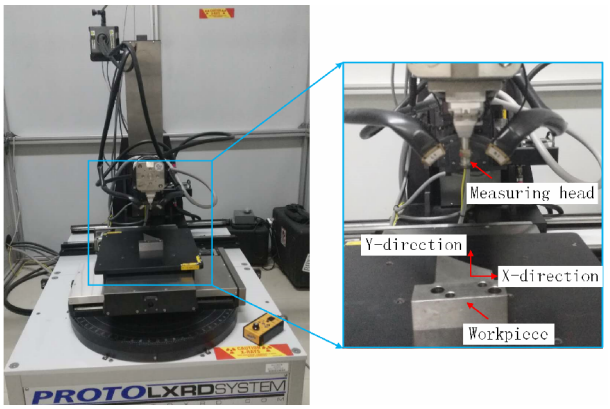

Fig. 9. LXRD MG2000 residual stress test analysis system.

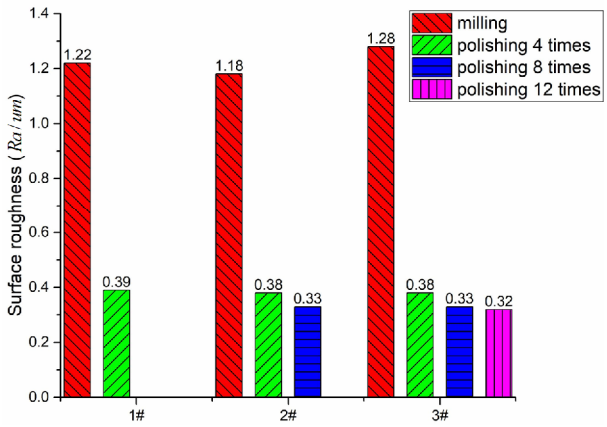

Fig. 10. Results of surface roughness measurement.

cutting section of the sample is then grinded and polished until the section becomes as smooth as a mirror in the metallographic grinding–polishing machine. The grinding process consists of coarse, semi-finished, and finished grinding. Second, five equidistant points in the grinded and polished cutting surfaces are selected to measure the micro-hardness. Third, micro-hardness is measured once by moving 5 μm under the surface until close to the body material's hardness to obtain the micro-hardness distribution in the depth direction. The test force is set to 25 gf, and the keeping load time is set to 6 s in the testing process. Finally, the average of these five values is calculated as the micro-hardness value of this point to meet the statistical significance of the measurement. PROTO LXRD MG2000 is also used as the micro-hardness measurement tool of the polished surface.

Microstructure. The microstructure of the cutting section is observed using TESCAN MIR3XMU field emission scanning electron microscopy. First, a sample of 10 mm × 10 mm × 2 mm on the blade processing area is cut, and the cutting section of the sample is grinded and polished until the section becomes as smooth as a mirror in the metallographic grinding–polishing machine. The cutting section is then corroded using corrosive liquid with the ratio of HCL:HNO_3:HF:H_2O = 3:5:2:100. Finally, the micro-structure of the cutting section is observed, and the enlargement factor is 1000 k.

5. Results and discussion

Surface roughness. Surface roughness can quantitatively characterize the microscopic roughness of the machined surface and is always an important indicator of surface integrity. The surface roughness value of the milled surface is larger that of the polished surface. This phenomenon is due to the tearing effect when the swarf is separated from the surface of the workpiece, and the tiny change of cutter in the milling process can result in a rugged workpiece surface. Large surface roughness easily leads to small cracks, which affect the use of the workpiece and reduce the life of aircraft engine. Hence, controlling the surface roughness is a major goal of polishing, and the surface roughness is also the main optimization goal in the current polishing parameters. As the final process of aero-engine blade forming, polishing process has a clear control requirement, that is, the surface roughness should be less than Ra 0.4 μm. Fig. 10 shows the results of surface roughness measurement. After milling, the surface roughness of 1#, 2# and 3# specimens are Ra 1.22, Ra 1.18, and Ra 1.28 μm, and the surface roughness of the specimens before polishing is in the range of Ra 1.0–1.4 μm. After polishing, the surface roughness of 1#, 2# and 3# specimens are Ra 0.39, Ra 0.33 and Ra 0.32 μm, and the difference in surface roughness between the two adjacent levels are 0.06 μm and 0.01 μm. The polishing target is that the surface roughness should be less than Ra 0.40 μm for the automatic polishing of aero-engine blade.

On the basis of the above analysis, the polishing goal can be achieved using the flexible adaptive polishing. That is, if the surface roughness of specimens before polishing is within the range of Ra 1.0–Ra 1.4 μm, then the surface roughness of the specimens can be reduced to less than Ra 0.40 by polishing four times by adopting the flexible process.

The surface roughness is reduced by 0.05 μm by polishing 8 times compared with 4 times and reduced by 0.01 μm by polishing 12 times compared with 8 times (Fig. 10). Therefore, the surface roughness will not change after polishing four times. Particularly, the polished surface roughness will not change after a certain number of polishing times. The number of polishing times directly affects the polishing efficiency. Therefore, the number of polishing times should be arranged within a reasonable range to improve the flexible polishing efficiency.

The blade consists of a rabbet, blade root, and blade body and is classified into concave and convex. The concave and convex blades are the main polishing parts. The experimental results show that convex manual polishing will require at least 30 minutes to finish. The concave manual polishing, which is more complicated compared with the convex one, will require at least 90 minutes to finish. The repeated manual detection and repair will cost additional time. Therefore, manual blade polishing will require 3 hours to finish. However, with flexible

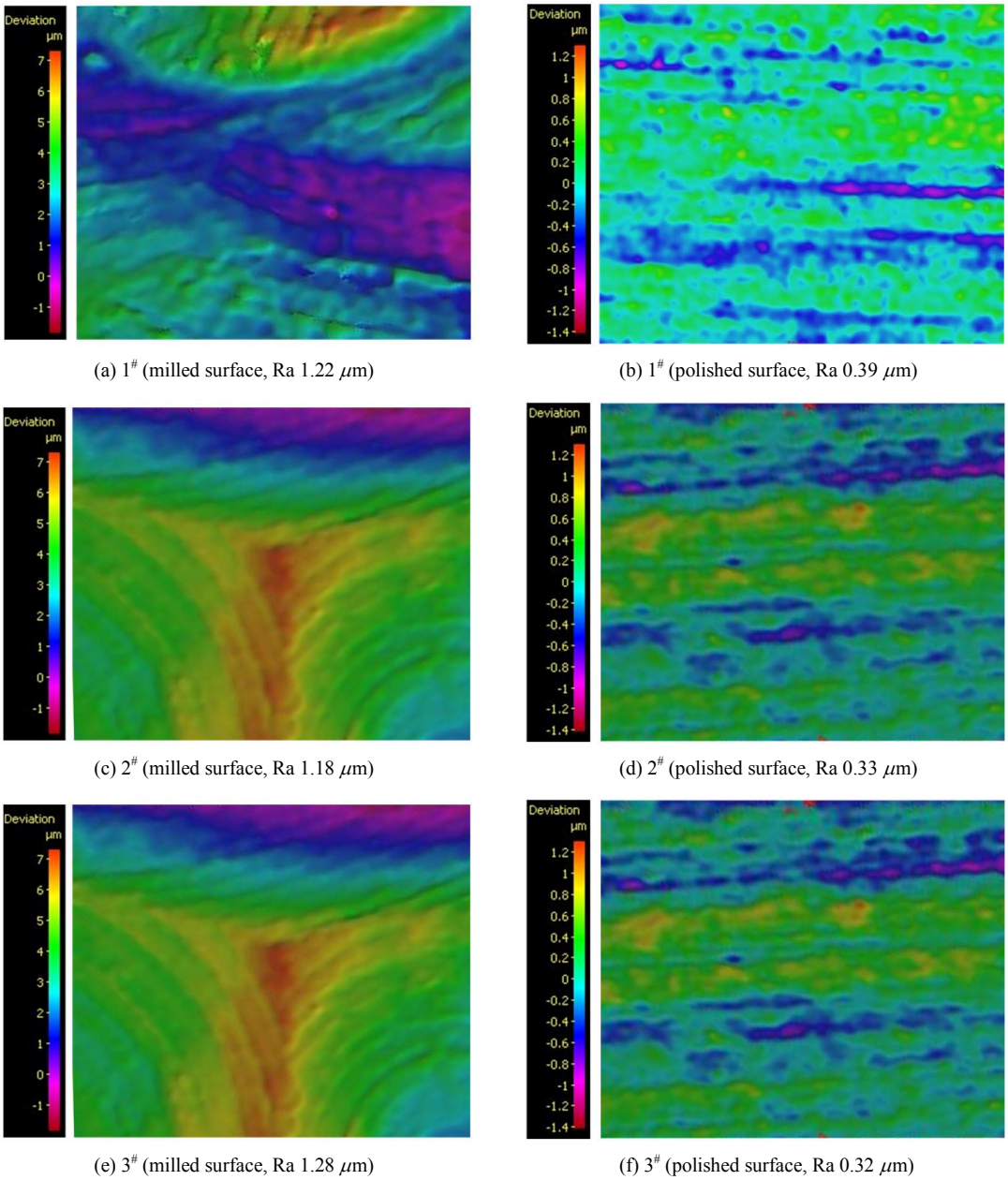

(a) 1# (milled surface, Ra 1.22 μm)

(b) 1# (polished surface, Ra 0.39 μm)

(c) 2# (milled surface, Ra 1.18 μm)

(d) 2# (polished surface, Ra 0.33 μm)

(e) 3# (milled surface, Ra 1.28 μm)

(f) 3# (polished surface, Ra 0.32 μm)

Fig. 11. Results of surface topography measurement.

adaptive polishing, the polishing will only require 45 minutes at most to finish. Flexible polishing is four times more efficient than manual polishing. Polishing efficiency will be higher if speed and feed speed are increased by optimizing the process parameters. According to the process plan, the final speed and feed speed will reach to 20000 rpm and 800 mm/min, respectively, and will require 14 minutes at most to finish the blade polishing. Therefore, the efficiency is high.

The experimental results show that the flexible polishing process is reliable; the value of surface roughness is reduced by approximately 77 % using this flexible polishing process. The surface roughness of the specimen significantly declines after being polished; the process can achieve polishing target; the number of polishing times has no effect on surface roughness, and the efficiency is high. The reduction of surface roughness can improve the corrosion resistance, fatigue strength, and contact stiffness of the blade, increasingly improve the vibration and noise performance of the blade, and improve the performance of the aero-engine.

Surface topography. Fig. 11 shows the surface topography, which is perpendicular to the flow direction of the blade. Fig. 11(a) shows the processing surface texture, which is the milled surface topography, and Fig. 11(b) shows the smooth surface, which is the polished surface topography. A significant change is observed in Figs. 11(a) and (b). The maximum peak value of the milled specimen surface is 7 μm; the bulge is

noticeable, and the pits in the milled surface topography and the surface are not flat. The maximum peak value of the polished specimen surface is 1.2 μm; the polished surface topography becomes smooth and flat, and the bulge and pits in the polished surface topography are not noticeable. The surface of polished specimen is noticeably deformed due to the squeezing of the polishing force, and the surface marks are difficult to recognize. The surface pits and unevenness have been significantly improved through the flexible polishing process; this process can effectively remove the knife marks, pits, unevenness, and other milling phenomena of the blade surface.

The milled surface topography of 1#, 2# and 3# specimens are shown in Figs. 11(a), (c) and (e), respectively. These specimens can be polished via flexible polishing process, whose roughness is in the range of Ra 1.0–1.4 μm and satisfies the requirement. An obvious changing rule does not exist in the milled surface topography which is less consistent and peculiar. The surface is not flat and noticeable bulges and pits exist. This finding is due to the large mechanical vibration, changes in tool temperature, material deformation, and other random factors in the milling process. The process makes the blade surface material produce temperature and shape changes, which result in significant defects in surface integrity.

The polished surface topography of 1#, 2# and 3# specimens are shown in Figs. 11(b), (d) and (f), respectively. The number of polishing times on the surface topography has a minimal effect under the same polishing process, and the surface topography will no longer change when the number of polishing times is achieved at a certain degree. Hence, the number of polishing times should be reasonably planned to improve the polishing efficiency.

The polished surface topography of the specimens is consistent compared with the different surface topographies obtained via milling. This result is caused by the abrasive cloth wheel possessing good flexibility, and the flexible polishing mechanism exhibits good self-adaptability and controllability; the polishing process can be changed based on the shape of the workpiece; the flexible polishing is a micro-grinding process, and the grinding heat and force are extremely small to improve the surface integrity defects generated during milling. The flexible polishing process achieves a good surface topography.

On the basis of the above analysis, the following conclusions can be drawn. Flexible polishing can effectively remove the knife marks, pits, unevenness, and other milling phenomenon of blade surface; the polished surface topography of specimens is consistent via the flexible polishing process compared with the different surface topographies obtained via milling, and this flexible polishing process can optimize the surface topography; the surface topography will no longer change when the number of polishing times is achieved at a certain degree.

Residual stress. The surface residual stresses of 1#, 2# and 3# specimens are shown in Fig. 12. Figs. 12(a) and (b) show the surface residual stress distributions of the x-direction, which is perpendicular to the stacking axis, and y-direction, which is along the stacking axis, respectively.

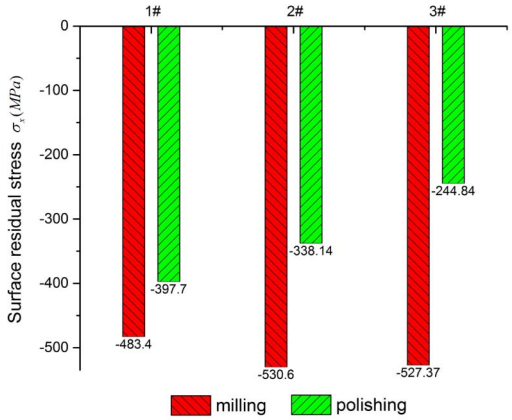

(a) Surface residual stress in X-direction

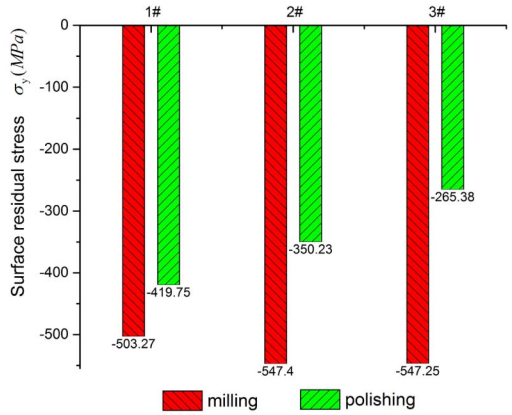

(b) Surface residual stress in Y-direction

Fig. 12. Results of surface residual stress measurement.

The milled surface residual stress in the x-direction is a residual compressive stress and is distributed around −510 MPa. The polished surface residual stress is also a residual compressive stress. The polished surface residual compressive stress values of 1#, 2# and 3# specimens are reduced by 86, 192 and 283 MPa, respectively, in comparison with the milled surface residual compressive stress. With the increase in the number of polishing times, the surface residual stress in the x-direction is reduced by a certain percentage. That is, the number of polishing times increases by four times, and the surface residual compressive is reduced by about 90 MPa. The milled surface residual stress in the y-direction is a residual compressive stress and is distributed around −500 MPa. The polished surface residual stress is also a residual compressive stress. The polished surface residual compressive stress values of 1#, 2# and 3# specimens are reduced by 94, 197 and 282 MPa, respectively. With the increase in the number of polishing times, the surface residual compressive stress in the y-direction of the polishing surface is almost the same as that of the x-direction.

The residual stress distribution along the depth of 1#, 2# and 3# specimens are shown in Figs. 13(a)-(c), respectively.

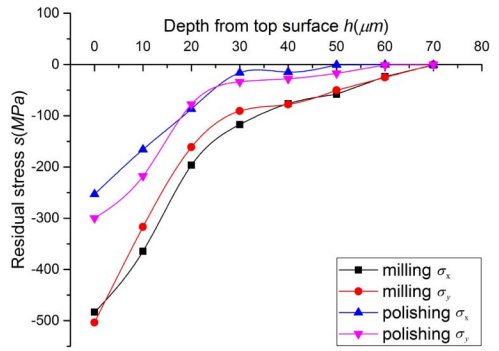

(a) 1#

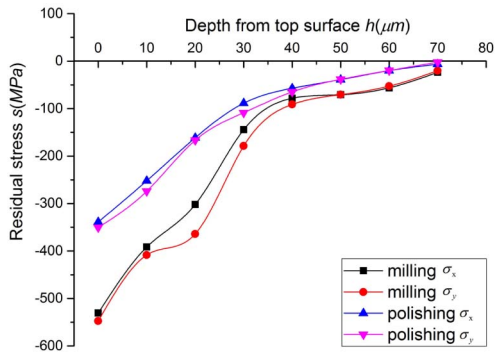

(b) 2#

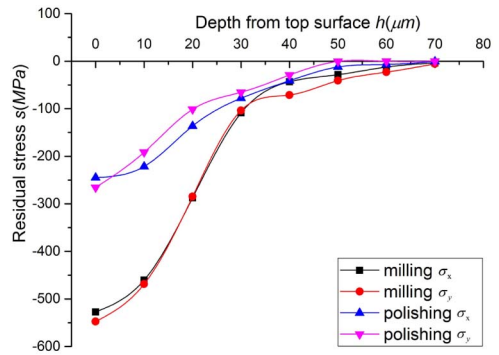

(c) 3#

Fig. 13. Residual stress distribution along the depth.

The residual stress is presented as residual compressive stress. The variation law of residual compressive stress distribution along the depth is basically the same. The figures show a decreasing tendency until the residual stress becomes the residual stress of the matrix at the depth of about 70 μm layers.

The specimen surface is consistently covered by wear particle group of the abrasive cloth wheel and the continuous friction; rolling and collision in the grinding process will release the surface residual stress, which reduces the value of surface residual stress. With the increase in the number of polishing times, the effects of friction, rolling, and collision will be critical. In addition, with the increase in the number of polishing times, the material removal amount of the workpiece will be larger, and the workpiece surface will be closer to the material matrix, in which the residual stress is close to 0 MPa. Thus, with the increase in the number of polishing times, the surface residual stress is reduced by a certain percentage. However, flexible polishing is a small grinding process, and the grinding force and heat are so extremely small that they cannot produce residual stress. The small polishing force and temperature result in small thermal–mechanical coupling effect, which does not affect the depth layer and no polishing burns and other workpiece destructions are observed. Flexible polishing can change the surface residual stress; however, the deep residual stress of the workpiece has no effect.

The following conclusions can be drawn for the residual stress. Flexible polishing process can change and reduce the surface residual compressive stress; the number of polishing times has a significant influence on the surface residual stress; with the increase in the number of polishing times, the surface residual stress decreases and the depth direction does not change. That is, the increase in the number of polishing times will affect the surface residual stress, thereby influencing the workpiece fatigue life. Therefore, the number of polishing times should be reasonably arranged to make the surface residual stress meet the scope of polishing requirements.

Micro-hardness. The micro-hardness of 1#, 2# and 3# specimens are shown in Figs. 14(a)-(c), respectively. A reading error associated with the diagonal length measurement due to the existing of indent always exists. The test error is ±10 HV, and fluctuations within the error can be ignored. The micro-hardness measured in the range of 5 μm below the surface is considerably smaller than the surface micro-hardness, which is caused by the boundary effect at the time of measurement. The micro-hardness of the polished specimen is higher than the milled specimen, and the growth trend of micro-hardness is similar in the different number of polishing times. Surface micro-hardness increases by 18, 22 and 24 HV. In addition, the curve of micro-hardness distribution along the depth is unchanged, and the change rule is the same as the milled specimen. This result is caused by the impact, squeeze, friction, and temperature changes used by the emery cloth wheel, which have a large effect on the specimen surface micro-hardness. In addition, the small polishing force and temperature result in minimal thermal–mechanical coupling effect, which does not affect the micro-hardness distribution along the depth.

The following conclusions can be drawn for the micro-hardness. The flexible polishing can increase the surface micro-hardness of the workpiece; the number of polishing times does not affect the surface micro-hardness and the change rule of micro-hardness distribution along the depth. Therefore, increasing the number of polishing times to improve the surface micro-hardness, which results in a reduction in the polishing efficiency is unnecessary.

Microstructure. The cross-section microstructure of 1#, 2# and 3# milled specimens are shown in Figs. 15(a), (c) and (e), respectively, and the cross-section microstructure of 1#, 2# and 3# polished specimens are shown in Figs. 15(b), (d) and (f), respectively. The internal grain of the surface material is

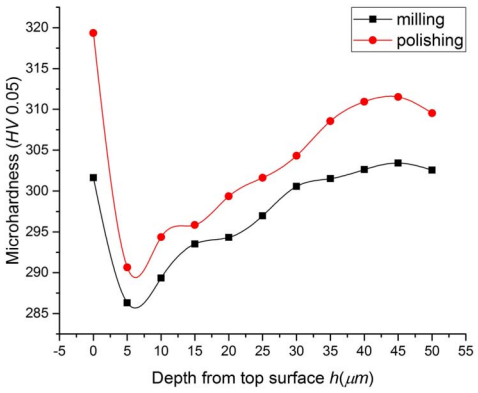

(a) 1#

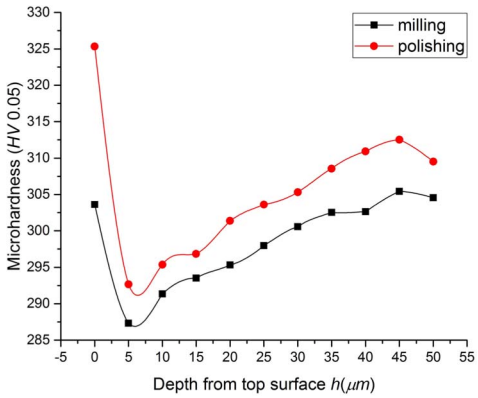

(b) 2#

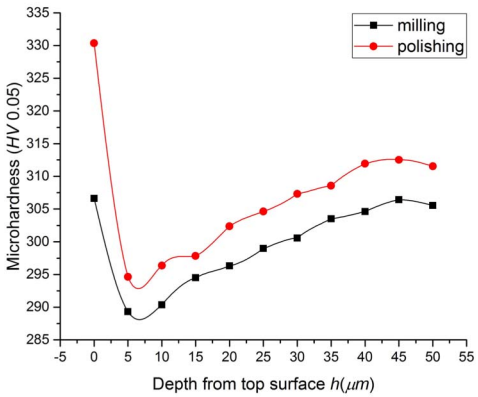

(c) 3#

Fig. 14. Micro-hardness distribution along the depth.

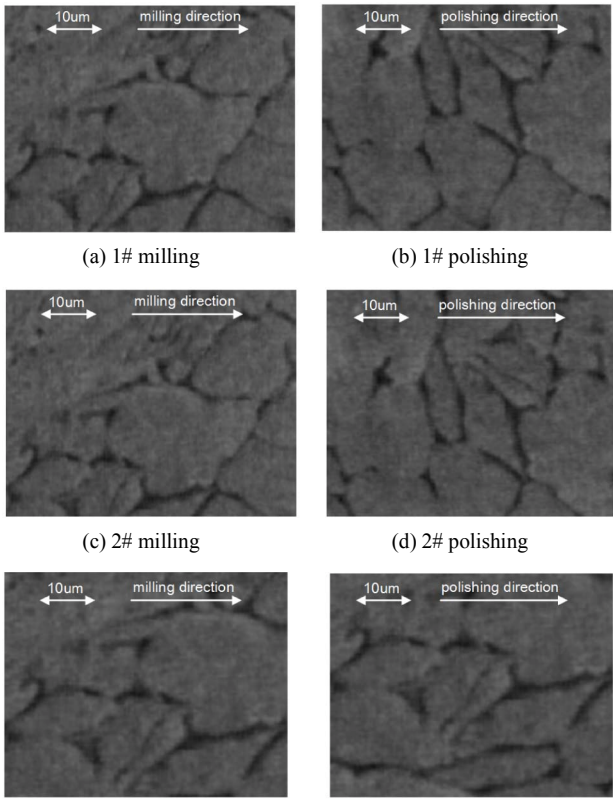

(a) 1# milling (b) 1# polishing

(c) 2# milling (d) 2# polishing

(e) 3# milling (f) 3# polishing

Fig. 15. Cross-section microstructure of the samples before and after flexible polishing.

compressed and slipped, which results in twisting, elongating, breaking, and other devastating changes in the milling process due to the violent friction between the cutter and workpiece, high-speed deformation, and high cutting heat. Flexible polishing is a micro-grinding process; thus, the grinding force and temperature are extremely small, which results in no layer deterioration and no phase change in the surface material. Flexible polishing process can remove the surface metamorphic layer, which is formed in the milling process and is different from the original property of the specimen material, with regard to its physical aspect, chemical property, and organizational structure. This process makes the workpiece surface material structure close to the workpiece matrix and restores the original surface material property. With the increase in the number of polishing times, the improvement of the surface metamorphic layer is not noticeable and the microstructure of the specimen cannot change.

The following conclusions can be drawn for the microstructure. Flexible polishing does not cause phase change and can remove the milled workpiece surface deterioration layer and make the material be closer to the workpiece base material; the increase in the number of polishing times cannot affect the surface metamorphic layer. Therefore, increasing the number of polishing times to improve the microstructure, which results in a reduction in the polishing efficiency, is unnecessary.

6. Conclusion

In this work, surface roughness, surface topography, residual stress, micro-hardness, and microstructure were investigated during the milling and polishing of TC4 titanium alloy blade. The results can be summarized as follows.

(1) TC4 titanium alloy blade was efficiently polished using the 5-axis 5-linkage flexible CNC polishing machine tool that the authors researched and developed based on the analysis of polishing process and surface integrity. Flexible polishing machine tool could be used in polishing the blade with com-

plex surface.

(2) The abrasive cloth wheel exhibited good flexibility, and the flexible polishing machine exhibited good self-adaptability and controllability; the polishing process changed based on the shape of the workpiece; the flexible polishing was a micro-grinding process; and the heat and force of polishing had minimal effect on surface integrity, thereby generating less surface defects and obtaining a strong surface topography.

(3) Flexible polishing process was reliable; the value of surface roughness reduced by approximately 77 % and could be controlled to be less than Ra 0.40 μm using the process. Flexible polishing could effectively remove the knife marks, pits, unevenness, and other milling defects of the blade surface. The polished surface roughness and topography would not change even after a certain number of polish times.

(4) Flexible polishing affected the residual stress on the surface of the workpiece but not the residual stress in the depth direction. The surface residual stress reduced by a certain percentage with the increase in the number of polishing times; however, the depth direction did not change.

(5) Flexible polishing could increase the surface micro-hardness of the workpiece. The number of polishing times did not affect the surface micro-hardness and the change rule of micro-hardness distribution along the depth.

(6) Flexible polishing did not induce phase change and could remove the milled workpiece surface deterioration layer and make the material be closer to the workpiece base material. The increase in the number of polishing times did not affect the surface metamorphic layer.

The new polishing method, that is, flexible polishing, aided in efficiently polishing the TC4 titanium alloy blade in this study. The method has high application value in replacing the current manual polishing and is conducive to industrial automation. Flexible polishing process only changes the surface quality and has no effect on the residual stress, micro-hardness, and microstructure of the depth direction. The process only changes the surface roughness, surface morphology, and surface residual stress and do not damage the internal structure of the workpiece and is, therefore, a reliable way to improve surface quality and is a valuable engineering application for aero-engine blade polishing.

Acknowledgments

This work was supported by the National Science Foundation of China (No. 51675439).

References

[1] D. A. Axinte, M. Kritmanorot, M. Axinte and N. N. Z Gindy, Investigations on belt polishing of heat-resistant titanium alloys, *Journal of Materials Processing Technology,* 166 (3) (2005) 398-404.

[2] D. A. Axinte, J. Kwong and M. C. Kong, Workpiece surface integrity of Ti-6-4 heat-resistant alloy when employing different polishing methods, *Journal of Materials Processing Technology,* 209 (4) (2009) 1843-1852.

[3] J. Rech, G. Kermouche, C. Claudin, A. Khellouki and W. Grzesik, Modelling of the residual stresses induced by belt finishing on a AISI52100 hardened steel, *International Journal of Material Forming*, 208 (1) (2008) 567-570.

[4] H. Tam and H. Cheng, An investigation of the effects of the tool path on the removal of material in polishing, *Journal of Materials Processing Technology,* 210 (5) (2010) 807-818.

[5] T. C. Hung, S. H. Chang and C. C. Lin, Effects of abrasive particle size and tool surface irregularities on wear rates of work and tool in polishing processes, *Microelectronic Engineering,* 88 (9) (2011) 2981-2990.

[6] E. S. Lee, S. G. Lee, W. K. Choi and S. G. Choi, Study on the effect of various machining speeds on the wafer polishing process, *Journal of Mechanical Science and Technology,* 27 (10) (2013) 3155-3160.

[7] A. Jourani, M. Dursapt, H. Hamdi, J. Rach and H. Zahouani, Effect of the belt grinding on the surface texture: Modeling of the contact and abrasive wear, *Wear,* 259 (2005) 1137-1143.

[8] E. Brinksmeier, O. Riemer and A. Gessenharter, Finishing of structured surfaces by abrasive polishing, *Precision Engineering,* 30 (2006) 325-336.

[9] M. Bigerelle, D. Najjar and A. Iost, Multiscale functional analysis of wear: A fractal model of the grinding process, *Wear*, 258 (2005) 232-239.

[10] M. Bigerelle, A. Gautier, B. Hagege, J. Favergeon and B. Bounichane, Roughness characteristic length scales of belt finished surface, *Journal of Materials Processing Technology*, 209 (2009) 6103-6116.

[11] M. Bigerelle, A. Gautier and A. Iost, Roughness characteristic length scales of micro-machined surfaces: A multi-scale modeling, *Sensors & Actuators B Chemical,* 126 (2007) 126-137.

[12] M. Bigerelle, B. Hagege and M. E. Mansori, Mechanical modelling of micro-scale abrasion in super finish belt grinding, *Tribology International,* 41 (2008) 992-1001.

[13] H. Hamdi, H. Zahouani and J. M. Bergheau, Residual stresses computation in a grinding process, *Journal of Materials Processing Technology,* 147 (2004) 277-285.

[14] J. Yang, M. Odén, M. P. Johansson-Jõesaar and L. Llanes, Grinding effects on surface integrity and mechanical strength of WC-Co cemented carbides, *Procedia CIRP,* 13 (2014) 257-263.

[15] W. H. Ho, J. T. Tsai, B. T. Lin and J. H. Chou, Adaptive network-based fuzzy inference system for prediction of surface roughness in end milling process using hybrid Taguchi-genetic learning algorithm, *Expert Systems with Applications*, 36 (2) (2009) 3216-3222.

[16] X. Han, Investigation of the surface generation mechanism of mechanical polishing engineering ceramics using discrete element method, *Applied Physics A*, 116 (4) (2014) 1729-1739.

[17] S. Gierlings, F. Klocke, M. Brockmann and D. Veselovac,

Force-based temperature modeling for surface integrity prediction in broaching nickel-based alloys, *CIRP Conference on Surface Integrity,* 13 (2014) 314-319.

[18] Y. Huang, C. Q. Yang and Z. Huang, Experimental research on abrasive belt grinding for 304 stainless streel, *The Chinese Mechanical Engineering*, 22 (3) (2011) 291-295.

[19] S. M. Ji, M. S. Jin and X. Zhang, Novel gasbag polishing technique for free-form mold, Chinese, *Journal of Mechanical Engineering*, 43 (8) (2007) 2-6.

[20] L. W. Guo, L. G. Yang and Y. Chen, Influence of magnetic abrasive finishing technology on surface integrity of vane-integrated disk, *China Surface Engineering*, 26 (3) (2013) 0010-0015.

[21] X. C. Huang, D. H. Zhang, C. F. Yang and J. X. Ren, Effect of grinding parameters on surface integrity of GH4169 nickel-based spirally, *Journal of Aerospace Power*, 23 (3) (2013) 621-628.

[22] C. Yao, W. Zuo, D.Wu, J. Ren and D. Zhang, Control rules of surface integrity and formation of metamorphic layer in high-speed milling of 7055 aluminum alloy, *Journal of Engineering Manufacture*, 229 (2) (2015) 187-204.

[23] X. J. Lin, Y. Yang, G. Yang, Y. Gao, Y. Chen, M. Li and J. X. Liu, The research of flexible polishing technology of five-axis NC abrasive belt for blade surface, *Acta Aeronautical et Astronautical Sonica*, 36 (6) (2015) 2074-2082.

[24] J. H. Duan, Y. Y. Shi, J. F. Zhang, T. Dong and X. B. Li, Flexible polishing technology for blade of aviation engine, *Acta Aeronautical et Astronautical Sonica*, 33 (3) (2012) 573-578.

Xiaojun Lin is a Professor of Northwestern Polytechnical University, Xi'an, China. His research fields mainly include CAD/CAM and automation, high-efficiency NC machining, and adaptive polishing technologies for complex surfaces.

Dongbo Wu is currently studying in Northwestern Polytechnical University, Xi'an, China. His research fields mainly include CAD/CAM and automation, high-efficiency NC machining, and adaptive polishing technologies for complex surfaces.